

A Constrained ℓ_1 Minimization Approach to Sparse Precision Matrix Estimation

Tony CAI, Weidong LIU, and Xi LUO

This article proposes a constrained ℓ_1 minimization method for estimating a sparse inverse covariance matrix based on a sample of n iid p -variate random variables. The resulting estimator is shown to have a number of desirable properties. In particular, the rate of convergence between the estimator and the true s -sparse precision matrix under the spectral norm is $s\sqrt{\log p/n}$ when the population distribution has either exponential-type tails or polynomial-type tails. We present convergence rates under the elementwise ℓ_∞ norm and Frobenius norm. In addition, we consider graphical model selection. The procedure is easily implemented by linear programming. Numerical performance of the estimator is investigated using both simulated and real data. In particular, the procedure is applied to analyze a breast cancer dataset and is found to perform favorably compared with existing methods.

KEY WORDS: Covariance matrix; Frobenius norm; Gaussian graphical model; Precision matrix; Rate of convergence; Spectral norm.

1. INTRODUCTION

Estimation of a covariance matrix and its inverse is an important problem in many areas of statistical analysis; among the many interesting examples are principal components analysis, linear/quadratic discriminant analysis, and graphical models. Stable and accurate covariance estimation is becoming increasingly important in the high-dimensional setting where the dimension p can be much larger than the sample size n . In this setting, classical methods and results based on fixed p and large n are no longer applicable. An additional challenge in the high-dimensional setting is the high computational cost. It is important that estimation procedures be computationally effective so that they can be used in high-dimensional applications.

Let $\mathbf{X} = (X_1, \dots, X_p)^T$ be a p -variate random vector with covariance matrix Σ_0 and precision matrix $\Omega_0 := \Sigma_0^{-1}$. Given an independent and identically distributed random sample $\{\mathbf{X}_1, \dots, \mathbf{X}_n\}$ from the distribution of \mathbf{X} , the most natural estimator of Σ_0 is perhaps

$$\hat{\Sigma}_n = \frac{1}{n} \sum_{k=1}^n (\mathbf{X}_k - \bar{\mathbf{X}})(\mathbf{X}_k - \bar{\mathbf{X}})^T,$$

where $\bar{\mathbf{X}} = n^{-1} \sum_{k=1}^n \mathbf{X}_k$. However, $\hat{\Sigma}_n$ is singular if $p > n$ and thus is unstable for estimating Σ_0 , not to mention that its inverse cannot be used to estimate the precision matrix Ω_0 . To estimate the covariance matrix Σ_0 consistently, special structures are usually imposed, and various estimators have been introduced under these assumptions. When the variables exhibit a certain ordering structure, which is often the case for time series data, Bickel and Levina (2008a) proved that banding the sample covariance matrix leads to a consistent estimator. Cai, Zhang, and Zhou (2010) established the minimax rate of convergence and introduced a rate-optimal tapering estimator. El Karoui (2008)

and Bickel and Levina (2008b) proposed thresholding of the sample covariance matrix for estimating a class of sparse covariance matrices and obtained rates of convergence for the thresholding estimators.

Estimation of the precision matrix Ω_0 is more involved due to the lack of a natural pivotal estimator like $\hat{\Sigma}_n$. Assuming certain ordering structures, methods based on banding the Cholesky factor of the inverse have been proposed and studied (see, e.g., Wu and Pourahmadi 2003; Huang et al. 2006; Bickel and Levina 2008b). Penalized likelihood methods also have been introduced for estimating sparse precision matrices. In particular, the ℓ_1 penalized normal likelihood estimator and its variants, which we call ℓ_1 -MLE type estimators, have been considered by several authors (see, e.g., Yuan and Lin 2007; d'Aspremont, Banerjee, and El Ghaoui 2008; Friedman, Hastie, and Tibshirani 2008; Rothman et al. 2008). Convergence rates under the Frobenius norm loss were given by Rothman et al. (2008). Yuan (2009) derived the convergence rates for sub-Gaussian distributions. Under more restrictive conditions, such as mutual incoherence or irrepresentable conditions, Ravikumar et al. (2008) obtained the convergence rates in the elementwise ℓ_∞ norm and spectral norm. Nonconvex penalties, which are usually computationally more demanding, also have been considered under the same normal likelihood model. For example, Lam and Fan (2009) and Fan, Feng, and Wu (2009) considered penalizing the normal likelihood with the nonconvex SCAD penalty. The main goal is to ameliorate the bias problem due to ℓ_1 penalization.

A closely related problem is recovery of the support of the precision matrix, which is strongly connected to the selection of graphical models. To be more specific, let $G = (V, E)$ be a graph representing conditional independence relations between components of \mathbf{X} . The vertex set V has p components X_1, \dots, X_p , and the edge set E consists of ordered pairs (i, j) , where $(i, j) \in E$ if there is an edge between X_i and X_j . The edge between X_i and X_j is excluded from E if and only if X_i and X_j are independent given $(X_k, k \neq i, j)$. If $\mathbf{X} \sim N(\boldsymbol{\mu}_0, \Sigma_0)$, then the conditional independence between X_i and X_j given other variables is equivalent to $\omega_{ij}^0 = 0$, where we set $\Omega_0 = (\omega_{ij}^0)$. Thus, for Gaussian distributions, recovering the structure of the

Tony Cai is Dorothy Silberberg Professor, Department of Statistics, The Wharton School, University of Pennsylvania, Philadelphia, PA 19104 (E-mail: tcai@wharton.upenn.edu). Weidong Liu is Faculty Member, Department of Mathematics and Institute of Natural Sciences, Shanghai Jiao Tong University, China and Postdoctoral Fellow, Department of Statistics, The Wharton School, University of Pennsylvania, Philadelphia, PA 19104. Xi Luo is Postdoctoral Fellow, Department of Statistics, The Wharton School, University of Pennsylvania, Philadelphia, PA 19104. The research of Tony Cai and Weidong Liu was supported in part by NSF FRG grant DMS-0854973. We would like to thank the Associate Editor and two referees for their very helpful comments which have led to a better presentation of the paper.

graph G is equivalent to estimating the support of the precision matrix (Lauritzen 1996). Liu, Lafferty, and Wasserman (2009) recently showed that for a class of non-Gaussian distribution called nonparanormal distribution, the problem of estimating the graph also can be reduced to estimating the precision matrix. In an important article, Meinshausen and Bühlmann (2006) convincingly demonstrated a neighborhood selection approach to recovering the support of $\mathbf{\Omega}_0$ in a row-by-row fashion. Yuan (2009) replaced the lasso selection by a Dantzig-type modification, where first the ratios between the off-diagonal elements ω_{ij} and the corresponding diagonal element ω_{ii} were estimated for each row i and then the diagonal entries ω_{ii} were obtained given the estimated ratios. Convergence rates under the matrix ℓ_1 norm and spectral norm losses were established.

In this article, we study estimation of the precision matrix $\mathbf{\Omega}_0$ for both sparse and nonsparse matrices, without restricting to a specific sparsity pattern. We also consider graphical model selection. We introduce a new method of constrained ℓ_1 -minimization for inverse matrix estimation (CLIME). Rates of convergence in the spectral norm, as well as the elementwise ℓ_∞ norm and Frobenius norm, are established under weaker assumptions and shown to be faster than those given for the ℓ_1 -MLE estimators when the population distribution has polynomial-type tails. A matrix is called s -sparse if there are at most s nonzero elements on each row. We show that when $\mathbf{\Omega}_0$ is s -sparse and \mathbf{X} has either exponential-type or polynomial-type tails, the error between our estimator $\hat{\mathbf{\Omega}}$ and $\mathbf{\Omega}_0$ satisfies $\|\hat{\mathbf{\Omega}} - \mathbf{\Omega}_0\|_2 = O_P(s\sqrt{\log p/n})$ and $|\hat{\mathbf{\Omega}} - \mathbf{\Omega}_0|_\infty = O_P(\sqrt{\log p/n})$, where $\|\cdot\|_2$ and $|\cdot|_\infty$ are the spectral norm and elementwise ℓ_∞ norm, respectively. We discuss properties of the CLIME estimator for estimating banded precision matrices. The CLIME method also can be adopted for the selection of graphical models, with an additional thresholding step. The elementwise ℓ_∞ norm result is instrumental for graphical model selection.

Besides having desirable theoretical properties, the CLIME estimator is computationally very attractive for high-dimensional data. It can be obtained one column at a time by solving a linear program, and the resulting matrix estimator is formed by combining the vector solutions (after a simple symmetrization). No outer iterations are needed, and the algorithm is easily scalable. An R package of our method has been developed and is publicly available on the Web. Here we investigate the numerical performance of the estimator using both simulated and real data. In particular, we apply the procedure to analyze a breast cancer dataset. The results show that the procedure performs favorably compared with existing methods.

The rest of the article is organized as follows. In Section 2, after introducing basic notations and definitions, we present the CLIME estimator. We establish the theoretical properties, including the rates of convergence, in Section 3, and discuss graphical model selection in Section 4. We consider the numerical performance of the CLIME estimator in Section 5 through simulation studies and a real data analysis. We provide further discussions on the connections and differences between our results and those of related work in Section 6. We relegate the proofs of our main results to Section 7.

2. ESTIMATION VIA CONSTRAINED ℓ_1 MINIMIZATION

In the compressed sensing and high-dimensional linear regression literature, it is now well understood that constrained ℓ_1 minimization provides an effective way to reconstruct a sparse signal (see, e.g., Donoho, Elad, and Temlyakov 2006; Candès and Tao 2007). A particularly simple and elementary analysis of constrained ℓ_1 minimization methods was given by Cai, Wang, and Xu (2010). In this section, we introduce a method of constrained ℓ_1 minimization for inverse covariance matrix estimation. We begin with basic notations and definitions. Throughout, for a vector $\mathbf{a} = (a_1, \dots, a_p)^T \in \mathbb{R}^p$, we define $|\mathbf{a}|_1 = \sum_{j=1}^p |a_j|$ and $|\mathbf{a}|_2 = \sqrt{\sum_{j=1}^p a_j^2}$. For a matrix $\mathbf{A} = (a_{ij}) \in \mathbb{R}^{p \times q}$, we define the elementwise ℓ_∞ norm $|\mathbf{A}|_\infty = \max_{1 \leq i \leq p, 1 \leq j \leq q} |a_{ij}|$, the spectral norm $\|\mathbf{A}\|_2 = \sup_{|\mathbf{x}|_2 \leq 1} |\mathbf{A}\mathbf{x}|_2$, the matrix ℓ_1 norm $\|\mathbf{A}\|_{L_1} = \max_{1 \leq j \leq q} \sum_{i=1}^p |a_{ij}|$, the Frobenius norm $\|\mathbf{A}\|_F = \sqrt{\sum_{i,j} a_{ij}^2}$, and the elementwise ℓ_1 norm $\|\mathbf{A}\|_1 = \sum_{i=1}^p \sum_{j=1}^q |a_{i,j}|$. \mathbf{I} denotes a $p \times p$ identity matrix. For any two index sets T and T' and matrix \mathbf{A} , we use $\mathbf{A}_{TT'}$ to denote the $|T| \times |T'|$ matrix with rows and columns of \mathbf{A} indexed by T and T' , respectively. The notation $\mathbf{A} > 0$ indicates that \mathbf{A} is positive definite.

We now define our CLIME estimator. Let $\{\hat{\mathbf{\Omega}}_1\}$ be the solution set of the following optimization problem:

$$\begin{aligned} \min \|\mathbf{\Omega}\|_1 \quad \text{subject to:} \\ |\mathbf{\Sigma}_n \mathbf{\Omega} - \mathbf{I}|_\infty \leq \lambda_n, \quad \mathbf{\Omega} \in \mathbb{R}^{p \times p}, \end{aligned} \quad (1)$$

where λ_n is a tuning parameter. In (1), we do not impose the symmetry condition on $\mathbf{\Omega}$, and as a result the solution is not symmetric in general. The final CLIME estimator of $\mathbf{\Omega}_0$ is obtained by symmetrizing $\hat{\mathbf{\Omega}}_1$ as follows. Write $\hat{\mathbf{\Omega}}_1 = (\hat{\omega}_{ij}^1) = (\hat{\omega}_1^1, \dots, \hat{\omega}_p^1)$. The CLIME estimator $\hat{\mathbf{\Omega}}$ of $\mathbf{\Omega}_0$ is defined as

$$\begin{aligned} \hat{\mathbf{\Omega}} &= (\hat{\omega}_{ij}), \quad \text{where} \\ \hat{\omega}_{ij} &= \hat{\omega}_{ji} = \hat{\omega}_{ij}^1 I\{|\hat{\omega}_{ij}^1| \leq |\hat{\omega}_{ji}^1|\} + \hat{\omega}_{ji}^1 I\{|\hat{\omega}_{ij}^1| > |\hat{\omega}_{ji}^1|\}. \end{aligned} \quad (2)$$

In other words, between $\hat{\omega}_{ij}^1$ and $\hat{\omega}_{ji}^1$, we take the one with smaller magnitude. Clearly, $\hat{\mathbf{\Omega}}$ is a symmetric matrix; moreover, Theorem 1 shows that it is positive definite with high probability.

The convex program (1) can be further decomposed into p vector minimization problems. Let \mathbf{e}_i be a standard unit vector in \mathbb{R}^p with 1 in the i th coordinate and 0 in all other coordinates. For $1 \leq i \leq p$, let $\hat{\boldsymbol{\beta}}_i$ be the solution of the following convex optimization problem:

$$\min |\boldsymbol{\beta}|_1 \quad \text{subject to} \quad |\mathbf{\Sigma}_n \boldsymbol{\beta} - \mathbf{e}_i|_\infty \leq \lambda_n, \quad (3)$$

where $\boldsymbol{\beta}$ is a vector in \mathbb{R}^p . The following lemma shows that solving the optimization problem (1) is equivalent to solving the p optimization problems (3), that is, $\{\hat{\mathbf{\Omega}}_1\} = \{\hat{\mathbf{B}}\} := \{(\hat{\boldsymbol{\beta}}_1, \dots, \hat{\boldsymbol{\beta}}_p)\}$. This simple observation is useful for both implementation and technical analysis.

Lemma 1. Let $\{\hat{\mathbf{\Omega}}_1\}$ be the solution set of (1), and let $\{\hat{\mathbf{B}}\} := \{(\hat{\boldsymbol{\beta}}_1, \dots, \hat{\boldsymbol{\beta}}_p)\}$, where $\hat{\boldsymbol{\beta}}_i$ are solutions to (3) for $i = 1, \dots, p$. Then $\{\hat{\mathbf{\Omega}}_1\} = \{\hat{\mathbf{B}}\}$.

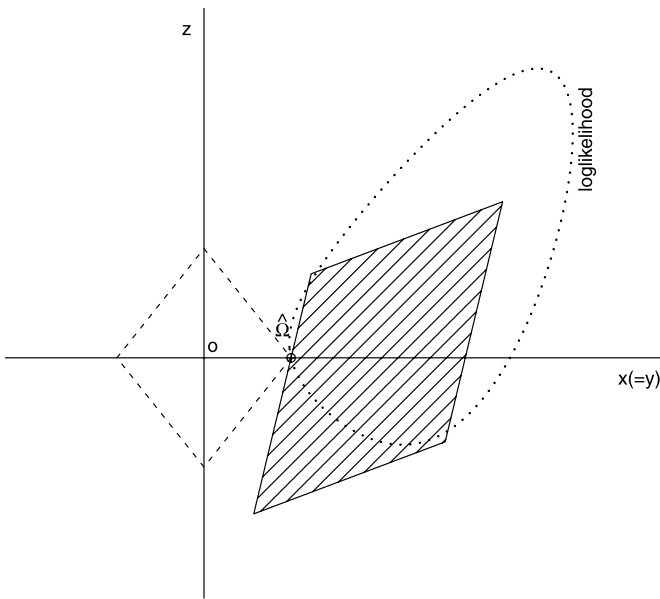


Figure 1. Plot of the elementwise ℓ_∞ constrained feasible set (shaded polygon) and the elementwise ℓ_1 norm objective (dashed diamond near the origin) from CLIME. The log-likelihood function as in Glasso is represented by the dotted line.

To illustrate the motivation of (1), let us recall the method based on ℓ_1 regularized log-determinant program (cf. Banerjee, Ghaoui, and d’Aspremont 2008; d’Aspremont, Banerjee, and El Ghaoui 2008; Friedman, Hastie, and Tibshirani 2008) as follows, which we call Glasso after the algorithm that efficiently computes the solution:

$$\hat{\Omega}_{\text{Glasso}} := \arg \min_{\Omega \succ 0} \{ \langle \Omega, \Sigma_n \rangle - \log \det(\Omega) + \lambda_n \|\Omega\|_1 \}. \quad (4)$$

The solution $\hat{\Omega}_{\text{Glasso}}$ satisfies

$$\hat{\Omega}_{\text{Glasso}}^{-1} - \Sigma_n = \lambda_n \hat{Z},$$

where \hat{Z} is an element of the subdifferential $\partial \|\hat{\Omega}_{\text{Glasso}}\|_1$. This leads us to consider the following optimization problem:

$$\begin{aligned} \min \|\Omega\|_1 \quad \text{subject to:} \\ \|\Omega^{-1} - \Sigma_n\|_\infty \leq \lambda_n, \quad \Omega \in \mathbb{R}^{p \times p}. \end{aligned} \quad (5)$$

However, the feasible set in (5) is very complicated. By multiplying the constraint with Ω , such a relaxation of (5) leads to the convex optimization problem (1), which can be solved easily. Figure 1 illustrates the solution for recovering a 2 by 2 precision matrix $\begin{bmatrix} x & z \\ z & y \end{bmatrix}$, and here we consider only the plane $x (= y)$ versus z for simplicity. The point where the feasible polygon meets the dashed diamond is the CLIME solution $\hat{\Omega}$. Note that here, as in Glasso, the log-likelihood function is a smooth curve, rather than the polygon constraint in CLIME.

3. RATES OF CONVERGENCE

In this section, we investigate the theoretical properties of the CLIME estimator and establish the rates of convergence under different norms. Write $\Sigma_n = (\hat{\sigma}_{ij}) = (\hat{\sigma}_1, \dots, \hat{\sigma}_p)$, $\Sigma_0 = (\sigma_{ij}^0)$, and $\mathbf{E}\mathbf{X} = (\mu_1, \dots, \mu_p)^T$. It is conventional to split the technical analysis into two cases according to the moment conditions on \mathbf{X} .

(C1) *Exponential-type tails:* Suppose that there exist some $0 < \eta < 1/4$ such that $\log p/n \leq \eta$ and

$$\mathbf{E}e^{t(X_i - \mu_i)^2} \leq K < \infty \quad \text{for all } |t| \leq \eta, \text{ for all } i,$$

where K is a bounded constant.

(C2) *Polynomial-type tails:* Suppose that for some $\gamma, c_1 > 0$, $p \leq c_1 n^\gamma$, and for some $\delta > 0$,

$$\mathbf{E}|X_i - \mu_i|^{4\gamma+4+\delta} \leq K \quad \text{for all } i.$$

For ℓ_1 -MLE type estimators, the convergence rates in the case of polynomial-type tails typically are much slower than those in the case of exponential-type tails (see, e.g., Ravikumar et al. 2008). We show that our CLIME estimator attains the same rates of convergence under either of the two moment conditions and significantly outperforms ℓ_1 -MLE type estimators in the case of polynomial-type tails.

3.1 Rates of Convergence Under Spectral Norm

We begin by considering the uniformity class of matrices,

$$\begin{aligned} \mathcal{U} &:= \mathcal{U}(q, s_0(p)) \\ &= \left\{ \Omega : \Omega \succ 0, \|\Omega\|_{L_1} \leq M, \max_{1 \leq i \leq p} \sum_{j=1}^p |\omega_{ij}|^q \leq s_0(p) \right\} \end{aligned}$$

for $0 \leq q < 1$, where $\Omega =: (\omega_{ij}) = (\omega_1, \dots, \omega_p)$. Similar parameter spaces were used by Bickel and Levina (2008b) to estimate the covariance matrix Σ_0 . Note that in the special case of $q = 0$, $\mathcal{U}(0, s_0(p))$ is a class of $s_0(p)$ -sparse matrices. Let

$$\theta = \max_{ij} \mathbf{E}[(X_i - \mu_i)(X_j - \mu_j) - \sigma_{ij}^0]^2 =: \max_{ij} \theta_{ij}.$$

The quantity θ_{ij} is related to the variance of $\hat{\sigma}_{ij}$, and the maximum value θ captures the overall variability of Σ_n . It is easy to see that under either (C1) or (C2), θ is a bounded constant depending only on γ, δ, K .

The following theorem gives the rates of convergence for the CLIME estimator $\hat{\Omega}$ under the spectral norm loss.

Theorem 1. Suppose that $\Omega_0 \in \mathcal{U}(q, s_0(p))$.

(a) Assume that (C1) holds. Let $\lambda_n = C_0 M \sqrt{\log p/n}$, where $C_0 = 2\eta^{-2}(2 + \tau + \eta^{-1}e^2 K^2)^2$ and $\tau > 0$. Then

$$\|\hat{\Omega} - \Omega_0\|_2 \leq C_1 M^{2-2q} s_0(p) \left(\frac{\log p}{n} \right)^{(1-q)/2}, \quad (6)$$

with probability greater than $1 - 4p^{-\tau}$, where $C_1 \leq 2(1 + 2^{1-q} + 3^{1-q})4^{1-q}C_0^{1-q}$.

(b) Assume that (C2) holds. Let $\lambda_n = C_2 M \sqrt{\log p/n}$, where $C_2 = \sqrt{(5 + \tau)(\theta + 1)}$. Then

$$\|\hat{\Omega} - \Omega_0\|_2 \leq C_3 M^{2-2q} s_0(p) \left(\frac{\log p}{n} \right)^{(1-q)/2}, \quad (7)$$

with probability greater than $1 - O(n^{-\delta/8} + p^{-\tau/2})$, where $C_3 \leq 2(1 + 2^{1-q} + 3^{1-q})4^{1-q}C_2^{1-q}$.

When M does not depend on n, p , the rates in Theorem 1 are the same as those used to estimate Σ_0 by Bickel and Levina (2008b). In the polynomial-type tails case and when $q = 0$, the rate in (7) is significantly better than the rate

$O(s_0(p)\sqrt{\frac{p^{1/(\gamma+1+\delta/4)}}{n}})$ for the ℓ_1 -MLE estimator obtained by Ravikumar et al. (2008).

It would be of great interest to get the convergence rates for $\sup_{\mathbf{\Omega}_0 \in \mathcal{U}} \mathbb{E} \|\hat{\mathbf{\Omega}} - \mathbf{\Omega}_0\|_2^2$. However, it is difficult even to prove the existence of the expectation of $\|\hat{\mathbf{\Omega}} - \mathbf{\Omega}_0\|_2^2$, because we are dealing with the inverse matrix. We modify the estimator $\hat{\mathbf{\Omega}}$ to ensure that such an expectation exists and the same rates are established. Let $\{\hat{\mathbf{\Omega}}_{1\rho}\}$ be the solution set of the following optimization problem:

$$\begin{aligned} \min \|\mathbf{\Omega}\|_1 \quad \text{subject to:} \\ |\mathbf{\Sigma}_{n,\rho}\mathbf{\Omega} - \mathbf{I}|_\infty \leq \lambda_n, \quad \mathbf{\Omega} \in \mathbb{R}^{p \times p}, \end{aligned} \quad (8)$$

where $\mathbf{\Sigma}_{n,\rho} = \mathbf{\Sigma}_n + \rho\mathbf{I}$ with $\rho > 0$. Write $\hat{\mathbf{\Omega}}_{1\rho} = (\hat{\omega}_{ij\rho}^1)$. Define the symmetrized estimator $\hat{\mathbf{\Omega}}_\rho$ as in (2) by

$$\begin{aligned} \hat{\mathbf{\Omega}}_\rho = (\hat{\omega}_{ij\rho}^1), \quad \text{where} \\ \hat{\omega}_{ij\rho}^1 = \hat{\omega}_{ji\rho}^1 = \hat{\omega}_{ij\rho}^1 I\{|\hat{\omega}_{ij\rho}^1| \leq |\hat{\omega}_{ji\rho}^1|\} + \hat{\omega}_{ji\rho}^1 I\{|\hat{\omega}_{ij\rho}^1| > |\hat{\omega}_{ji\rho}^1|\}. \end{aligned} \quad (9)$$

Clearly, $\mathbf{\Sigma}_{n,\rho}^{-1}$ is a feasible point, and thus we have $\|\hat{\mathbf{\Omega}}_{1\rho}\|_{L_1} \leq \|\mathbf{\Sigma}_{n,\rho}^{-1}\|_{L_1} \leq \rho^{-1}p$. The expectation $\mathbb{E}\|\hat{\mathbf{\Omega}}_\rho - \mathbf{\Omega}_0\|_2^2$ is then well defined. The other motivation to replace $\mathbf{\Sigma}_n$ with $\mathbf{\Sigma}_{n,\rho}$ comes from our implementation, which computes (1) by the primal dual interior point method. One usually needs to specify a feasible initialization. When $p > n$, it is hard to find an initial value for (1). For (8), we can simply set the initial value to $\mathbf{\Sigma}_{n,\rho}^{-1}$.

Theorem 2. Suppose that $\mathbf{\Omega}_0 \in \mathcal{U}(q, s_0(p))$ and (C1) holds. Let $\lambda_n = C_0 M \sqrt{\log p/n}$, with C_0 defined as in Theorem 1(a) and τ sufficiently large. Let $\rho = \sqrt{\log p/n}$. If $p \geq n^\xi$ for some $\xi > 0$, then we have

$$\sup_{\mathbf{\Omega}_0 \in \mathcal{U}} \mathbb{E} \|\hat{\mathbf{\Omega}}_\rho - \mathbf{\Omega}_0\|_2^2 = O\left(M^{4-4q} s_0^2(p) \left(\frac{\log p}{n}\right)^{1-q}\right).$$

Remark. It is not necessary to restrict $\rho = \sqrt{\log p/n}$. In fact, from the proof, we can see that Theorem 2 still holds for

$$\min\left(\sqrt{\frac{\log p}{n}}, p^{-\alpha}\right) \leq \rho \leq \sqrt{\frac{\log p}{n}} \quad (10)$$

with any $\alpha > 0$.

When the variables of \mathbf{X} are ordered, better rates can be obtained. Similar to Bickel and Levina (2008a), we consider the following class of precision matrices:

$$\begin{aligned} \mathcal{U}_o(\alpha, B) = \left\{ \mathbf{\Omega} : \mathbf{\Omega} > 0, \right. \\ \left. \max_j \sum_i \{|\omega_{ij}| : |i-j| \geq k\} \leq B(k+1)^{-\alpha} \right. \\ \left. \text{for all } k \geq 0 \right\} \end{aligned}$$

for $\alpha > 0$. Suppose that the modified Cholesky factor of $\mathbf{\Omega}_0$ is $\mathbf{\Omega}_0 = TD^{-1}T$, with the unique lower triangular matrix T and diagonal matrix D . To estimate $\mathbf{\Omega}_0$, Bickel and Levina (2008a) used the banding method and assumed $T \in \mathcal{U}_o(\alpha, B)$. It is easy to see that $T \in \mathcal{U}_o(\alpha, B)$ implies $\mathbf{\Omega}_0 \in \mathcal{U}_o(\alpha, B_1)$ for some constant B_1 . Rather than assuming $T \in \mathcal{U}_o(\alpha, B)$, we use a more general assumption that $\mathbf{\Omega}_0 \in \mathcal{U}_o(\alpha, B)$.

Theorem 3. Let $\mathbf{\Omega}_0 \in \mathcal{U}_o(\alpha, B)$ and $\lambda_n = CB\sqrt{\log p/n}$ with sufficiently large C .

(a) If (C1) or (C2) holds, then with probability greater than $1 - O(n^{-\delta/8} + p^{-\tau/2})$,

$$\|\hat{\mathbf{\Omega}} - \mathbf{\Omega}_0\|_2 = O\left(B^2 \left(\frac{\log p}{n}\right)^{\alpha/(2\alpha+2)}\right). \quad (11)$$

(b) Suppose that $p \geq n^\xi$ for some $\xi > 0$. If (C1) holds and $\rho = \sqrt{\log p/n}$, then

$$\sup_{\mathbf{\Omega}_0 \in \mathcal{U}_o(\alpha, B)} \mathbb{E} \|\hat{\mathbf{\Omega}}_\rho - \mathbf{\Omega}_0\|_2^2 = O\left(B^4 \left(\frac{\log p}{n}\right)^{\alpha/(\alpha+1)}\right). \quad (12)$$

Theorem 3 shows that our estimator has the same rate as that of Bickel and Levina (2008a) by banding the Cholesky factor of the precision matrix for the ordered variables.

3.2 Rates Under the l_∞ Norm and Frobenius Norm

So far, we have focused on the performance of the estimator under the spectral norm loss. Rates of convergence also can be obtained under the elementwise l_∞ norm and the Frobenius norm.

Theorem 4. (a) Under the conditions of Theorem 1(a), we have

$$|\hat{\mathbf{\Omega}} - \mathbf{\Omega}_0|_\infty \leq 4C_0 M^2 \sqrt{\frac{\log p}{n}},$$

$$\frac{1}{p} \|\hat{\mathbf{\Omega}} - \mathbf{\Omega}_0\|_F^2 \leq 4C_1 M^{4-2q} s_0(p) \left(\frac{\log p}{n}\right)^{1-q/2},$$

with probability greater than $1 - 4p^{-\tau}$.

(b) Under the conditions of Theorem 1(b), we have

$$|\hat{\mathbf{\Omega}} - \mathbf{\Omega}_0|_\infty \leq 4C_2 M^2 \sqrt{\frac{\log p}{n}},$$

$$\frac{1}{p} \|\hat{\mathbf{\Omega}} - \mathbf{\Omega}_0\|_F^2 \leq 4C_3 M^{4-2q} s_0(p) \left(\frac{\log p}{n}\right)^{1-q/2},$$

with probability greater than $1 - O(n^{-\delta/8} + p^{-\tau/2})$.

The rate in Theorem 4(b) is significantly faster than the rate obtained by Ravikumar et al. (2008); see Section 3.3 for more detailed discussion. A similar rate to ours was obtained by Lam and Fan (2009) under the Frobenius norm. The elementwise ℓ_∞ norm result will lead to the model selection consistency result that we present in the next section. We now give the rates for $\hat{\mathbf{\Omega}}_\rho - \mathbf{\Omega}_0$ under expectation.

Theorem 5. Under the conditions of Theorem 2, we have

$$\sup_{\mathbf{\Omega}_0 \in \mathcal{U}} \mathbb{E} |\hat{\mathbf{\Omega}}_\rho - \mathbf{\Omega}_0|_\infty^2 = O\left(M^4 \frac{\log p}{n}\right),$$

$$\frac{1}{p} \sup_{\mathbf{\Omega}_0 \in \mathcal{U}} \mathbb{E} \|\hat{\mathbf{\Omega}}_\rho - \mathbf{\Omega}_0\|_F^2 = O\left(M^{4-2q} s_0(p) \left(\frac{\log p}{n}\right)^{1-q/2}\right).$$

The proofs of Theorems 1–5 rely on the following more general theorem.

Theorem 6. Suppose that $\mathbf{\Omega}_0 \in \mathcal{U}(q, s_0(p))$ and $\rho \geq 0$. If $\lambda_n \geq \|\mathbf{\Omega}_0\|_{L_1} (\max_{ij} |\hat{\sigma}_{ij} - \sigma_{ij}^0| + \rho)$, then we have

$$\|\hat{\mathbf{\Omega}}_\rho - \mathbf{\Omega}_0\|_\infty \leq 4\|\mathbf{\Omega}_0\|_{L_1} \lambda_n, \tag{13}$$

$$\|\hat{\mathbf{\Omega}}_\rho - \mathbf{\Omega}_0\|_2 \leq C_4 s_0(p) \lambda_n^{1-q}, \tag{14}$$

and

$$\frac{1}{p} \|\hat{\mathbf{\Omega}}_\rho - \mathbf{\Omega}_0\|_F^2 \leq C_5 s_0(p) \lambda_n^{2-q}, \tag{15}$$

where $C_4 \leq 2(1 + 2^{1-q} + 3^{1-q})(4\|\mathbf{\Omega}_0\|_{L_1})^{1-q}$ and $C_5 \leq 4\|\mathbf{\Omega}_0\|_{L_1} C_4$.

3.3 Comparison With the Lasso-Type Estimator

Here we compare our results with those of Ravikumar et al. (2008), who estimated $\mathbf{\Omega}_0$ by solving the following ℓ_1 regularized log-determinant program:

$$\hat{\mathbf{\Omega}}_\star := \arg \min_{\Theta > 0} \{ \langle \mathbf{\Omega}, \mathbf{\Sigma}_n \rangle - \log \det(\mathbf{\Omega}) + \lambda_n \|\mathbf{\Omega}\|_{1,\text{off}} \}, \tag{16}$$

where $\|\mathbf{\Omega}\|_{1,\text{off}} = \sum_{i \neq j} |\omega_{ij}|$. To obtain the rates of convergence in the elementwise ℓ_∞ norm and the spectral norm, they imposed the following condition:

Irrepresentable Condition in Ravikumar et al. (2008). There exists some $\alpha \in (0, 1]$ such that

$$\|\mathbf{\Gamma}_{S^c S}(\mathbf{\Gamma}_{SS})^{-1}\|_{L_1} \leq 1 - \alpha, \tag{17}$$

where $\mathbf{\Gamma} = \mathbf{\Sigma}_0^{-1} \otimes \mathbf{\Sigma}_0^{-1}$, S is the support of $\mathbf{\Omega}_0$ and $S^c = \{1, \dots, p\} \times \{1, \dots, p\} - S$.

The foregoing assumption is particularly strong. Under this assumption, Ravikumar et al. (2008) showed that $\hat{\mathbf{\Omega}}_\star$ estimates the zero elements of $\mathbf{\Omega}_0$ exactly by 0 with high probability. In fact, a similar condition to (17) for Lasso with the covariance matrix $\mathbf{\Sigma}_0$ taking the place of the matrix $\mathbf{\Gamma}$ is sufficient and nearly necessary for recovering the support using the ordinary Lasso (see, e.g., Meinshausen and Bühlmann 2006).

Suppose that $\mathbf{\Omega}_0$ is $s_0(p)$ -sparse and consider sub-Gaussian random variables $X_i/\sqrt{\sigma_{ii}^0}$ with the parameter σ . In addition to (17), Ravikumar et al. (2008) assumed that the sample size n satisfies the bound

$$n > C_1 s_0^2(p) (1 + 8/\alpha)^2 (\tau \log p + \log 4), \tag{18}$$

where $C_1 = \{48\sqrt{2}(1 + 4\sigma^2) \max_i(\sigma_{ii}^0) \max\{\|\mathbf{\Sigma}_0\|_{L_1} K_\Gamma, \|\mathbf{\Sigma}_0\|_{L_1}^3 K_\Gamma^2\}\}^2$. Under the aforementioned conditions, they showed that with probability greater than $1 - 1/p^{\tau-2}$,

$$\begin{aligned} \|\hat{\mathbf{\Omega}}_\star - \mathbf{\Omega}_0\|_\infty \leq & \left\{ 16\sqrt{2}(1 + 4\sigma^2) \max_i(\sigma_{ii}) (1 + 8\alpha^{-1}) K_\Gamma \right\} \\ & \times \sqrt{\frac{\tau \log p + \log 4}{n}}, \end{aligned}$$

where $K_\Gamma = \|([\mathbf{\Sigma}_0 \otimes \mathbf{\Sigma}_0]_{SS})^{-1}\|_{L_1}$. Note that their constant depends on quantities α and K_Γ , whereas our constant depends on M , the bound of $\|\mathbf{\Omega}_0\|_{L_1}$. They required (18), whereas we need only $\log p = o(n)$. Another substantial difference is that the irrepresentable condition (17) is not needed for our results.

We next compare our result with that of Ravikumar et al. (2008) under the case of polynomial-type tails. Suppose that (C2) holds. Corollary 2 of Ravikumar et al. (2008) shows that if $p = O(\{n/s_0^2(p)\}^{(\gamma+1+\delta/4)/\tau})$ for some $\tau > 2$, then with probability greater than $1 - 1/p^{\tau-2}$,

$$\|\hat{\mathbf{\Omega}}_\star - \mathbf{\Omega}_0\|_\infty = O\left(\sqrt{\frac{p^{\tau/(\gamma+1+\delta/4)}}{n}}\right).$$

Theorem 4 shows that our estimator still has the order of $\sqrt{\log p/n}$ in the case of polynomial-type tails. Moreover, when $\gamma \geq 1$, the range $p = O(n^\gamma)$ in our theorem is wider than their range $p = O(\{n/s_0^2(p)\}^{(\gamma+1+\delta/4)/\tau})$ with $\tau > 2$.

It is worth noting that our estimator allows for a wider class of matrices compared with the sparse precision matrices. For example, the estimator is still consistent for the model, which is not truly sparse but has many small entries.

4. GRAPHICAL MODEL SELECTION CONSISTENCY

As mentioned in the Introduction, graphical model selection is an important problem. The constrained ℓ_1 minimization procedure introduced in Section 2 for estimating $\mathbf{\Omega}_0$ can be modified to recover the support of $\mathbf{\Omega}_0$. We introduce an additional thresholding step based on $\hat{\mathbf{\Omega}}$. More specifically, define a threshold estimator $\tilde{\mathbf{\Omega}} = (\tilde{\omega}_{ij})$ with

$$\tilde{\omega}_{ij} = \hat{\omega}_{ij} I\{|\hat{\omega}_{ij}| \geq \tau_n\},$$

where $\tau_n \geq 4M\lambda_n$ is a tuning parameter and λ_n is given in Theorem 1.

Define

$$\mathcal{M}(\tilde{\mathbf{\Omega}}) = \{\text{sgn}(\tilde{\omega}_{ij}), 1 \leq i, j \leq p\},$$

$$\mathcal{M}(\mathbf{\Omega}_0) = \{\text{sgn}(\omega_{ij}^0), 1 \leq i, j \leq p\},$$

$$S(\mathbf{\Omega}_0) = \{(i, j) : \omega_{ij}^0 \neq 0\},$$

and

$$\theta_{\min} = \min_{(i,j) \in S(\mathbf{\Omega}_0)} |\omega_{ij}^0|.$$

From the elementwise ℓ_∞ results established in Theorem 4, with high probability, the resulting elements in $\tilde{\mathbf{\Omega}}$ will exceed the threshold level if the corresponding element in $\mathbf{\Omega}_0$ is large in magnitude. In contrast, the elements of $\tilde{\mathbf{\Omega}}$ outside the support of $\mathbf{\Omega}_0$ will remain below the threshold level with high probability. Therefore, we have the following theorem on the threshold estimator $\tilde{\mathbf{\Omega}}$.

Theorem 7. Suppose that (C1) or (C2) holds and $\mathbf{\Omega}_0 \in \mathcal{U}(0, s_0(p))$. If $\theta_{\min} > 2\tau_n$, then, with probability greater than $1 - O(n^{-\delta/8} + p^{-\tau/2})$, we have $\mathcal{M}(\tilde{\mathbf{\Omega}}) = \mathcal{M}(\mathbf{\Omega}_0)$.

The threshold estimator $\tilde{\mathbf{\Omega}}$ recovers not only the sparsity pattern of $\mathbf{\Omega}_0$, but also the signs of the nonzero elements. This property is called sign consistency in some of the literature.

The condition $\theta_{\min} > 2\tau_n$ is needed to ensure that nonzero elements are correctly retained. From Theorem 4, we see that if M does not depend on n, p , then τ_n is of order $\sqrt{\log p/n}$, which is of the same order as in the assumption of Ravikumar et al. (2008) for exponential-type tails, but weaker than in their assumption $\theta_{\min} \geq C\sqrt{\frac{p^{\tau/(\gamma+1+\delta/4)}}{n}}$ for polynomial-type tails.

Based on Meinshausen and Bühlmann (2006), Zhou, van de Geer, and Bühlmann (2009) applied the adaptive Lasso to covariance selection in Gaussian graphical models. For $\mathbf{X} = (X_1, \dots, X_p)^T \sim \mathbf{N}(\mathbf{0}, \boldsymbol{\Sigma}_0)$, they regressed X_i versus the other variables $\{X_k; k \neq i\}$: $X_i = \sum_{j \neq i} \beta_j^i X_j + V_i$, where V_i is a normally distributed random variable with mean 0 and the underlying coefficients can be shown to be $\beta_j^i = -\omega_{ij}^0/\omega_{ii}^0$. They then used the adaptive Lasso to recover the support of $\{\beta_j^i\}$, which is identical to the support of $\boldsymbol{\Omega}_0$. One of their main assumptions is the restricted eigenvalue assumption on $\boldsymbol{\Sigma}_0$, which is weaker than the irrerepresentable condition. Their method can recover the support of $\boldsymbol{\Omega}_0$ but cannot estimate the elements in $\boldsymbol{\Omega}_0$. Besides not imposing the unnecessary irrerepresentable condition, an additional advantage of our method is that it not only recovers the support of $\boldsymbol{\Omega}_0$, but also provides consistency results under the elementwise l_∞ norm and the spectral norm.

5. NUMERICAL RESULTS

In this section, we turn to the numerical performance of our CLIME estimator. The procedure is easy to implement. An R package of our method has been developed and is available at <http://stat.wharton.upenn.edu/~tcail/paper/html/Precision-Matrix.html>. Here we first investigate the numerical performance of the estimator through simulation studies, and then apply our method to the analysis of a breast cancer dataset.

The proposed estimator $\hat{\boldsymbol{\Omega}}$ can be obtained in a column-by-column fashion as illustrated in Lemma 1. Thus we focus on the numerical implementation of solutions to the optimization problem (3):

$$\min \|\boldsymbol{\beta}\|_1 \quad \text{subject to:} \quad \|\boldsymbol{\Sigma}_n \boldsymbol{\beta} - \mathbf{e}_i\|_\infty \leq \lambda_n.$$

We consider relaxation of the foregoing, which is equivalent to the following linear programming problem:

$$\begin{aligned} \min \sum_{j=1}^p u_j \quad \text{subject to:} \\ -\beta_j \leq u_j \quad \text{for all } 1 \leq j \leq p, \\ +\beta_j \leq u_j \quad \text{for all } 1 \leq j \leq p, \\ -\hat{\boldsymbol{\sigma}}_k^T \boldsymbol{\beta} + I\{k=i\} \leq \lambda_n \quad \text{for all } 1 \leq k \leq p, \\ +\hat{\boldsymbol{\sigma}}_k^T \boldsymbol{\beta} - I\{k=i\} \leq \lambda_n \quad \text{for all } 1 \leq k \leq p. \end{aligned} \quad (19)$$

The same linear relaxation was considered by Candès and Tao (2007), who found it very efficient for the Dantzig selector problem in regression. To solve (19), we follow the primal dual interior method approach (see, e.g., Boyd and Vandenberghe 2004). The resulting algorithm has comparable numerical performance to other numerical procedures, including Glasso. Note that we need only sweep through the p columns once, but Glasso requires an extra outer layer of iterations to loop through the p columns several times by cyclical coordinate descent. Once $\hat{\boldsymbol{\Omega}}_1$ is obtained by combining the $\hat{\boldsymbol{\beta}}^i$'s for each column, we symmetrize $\hat{\boldsymbol{\Omega}}_1$ by setting the entry (i, j) to be the smaller in magnitude of two entries $\hat{\omega}_{ij}^1$ and $\hat{\omega}_{ji}^1$, for all $1 \leq i, j \leq p$, as in (2).

Similar to many iterative methods, our method also requires a proper initialization within the feasible set. However, the initializing $\boldsymbol{\beta}^0$ cannot simply be replaced by the solution of the

linear system $\boldsymbol{\Sigma}_n \boldsymbol{\beta} = \mathbf{e}_i$ for each i when $p > n$, because $\boldsymbol{\Sigma}_n$ is singular. The remedy is to add a small positive constant ρ (e.g., $\rho = \sqrt{\log p/n}$) to all of the diagonal entries of the matrix $\boldsymbol{\Sigma}_n$; that is, we use the ρ -perturbed matrix $\boldsymbol{\Sigma}_{n,\rho} = \boldsymbol{\Sigma}_n + \rho \mathbf{I}$ to replace the $\boldsymbol{\Sigma}_n$ in (19). Such a perturbation does not noticeably affect the computational accuracy of the final solution in our numerical experiments. In Sections 3 and 4, the resulting solution $\hat{\boldsymbol{\Omega}}_\rho$ in the perturbed problem (8) is shown to have all of the theoretical properties, and, even better, the convergence rate of the spectral norm under expectation is established for $\hat{\boldsymbol{\Omega}}_\rho$.

In the context of high-dimensional linear regression, a second-stage refitting procedure was considered by Candès and Tao (2007) to correct the biases introduced by the ℓ_1 norm penalization. Their refitting procedure seeks the best coefficient vector, giving the maximum likelihood, which has the same support as the original Dantzig selector. Inspired by this two-stage procedure, we propose a similar two-stage procedure to further improve the numerical performance of the CLIME estimator by refitting as

$$\check{\boldsymbol{\Omega}} = \arg \min_{\boldsymbol{\Omega}_{\hat{S}^c} = 0} \{ \langle \boldsymbol{\Omega}, \boldsymbol{\Sigma}_n \rangle - \log \det(\boldsymbol{\Omega}) \},$$

where $\hat{S} = S(\check{\boldsymbol{\Omega}})$ and $\boldsymbol{\Omega}_{\hat{S}^c} = \{\omega_{ij}, (i, j) \in \hat{S}^c\}$. Here the estimator $\check{\boldsymbol{\Omega}}$ minimizes the Bregman divergence among all symmetric positive definite matrices under the constraint. We call $\check{\boldsymbol{\Omega}}$ the refitted CLIME. We can establish the bounds under the three norms in Section 3 and the support recovery $S(\check{\boldsymbol{\Omega}}) = S(\boldsymbol{\Omega}_0)$. For example, the Frobenius loss bound can be easily derived from the approach used by Rothman et al. (2008) and Fan, Feng, and Wu (2009). Other theoretical properties are more involved, and we leave this to future work.

5.1 Simulations

Here we compare the numerical performance of the CLIME estimator $\hat{\boldsymbol{\Omega}}_{\text{CLIME}}$, the Refitted CLIME estimator, the Graphical Lasso $\hat{\boldsymbol{\Omega}}_{\text{Glasso}}$, and the SCAD $\hat{\boldsymbol{\Omega}}_{\text{SCAD}}$ from Fan, Feng, and Wu (2009), which is defined as

$$\hat{\boldsymbol{\Omega}}_{\text{SCAD}} := \arg \min_{\Theta > 0} \left\{ \langle \boldsymbol{\Omega}, \boldsymbol{\Sigma}_n \rangle - \log \det(\boldsymbol{\Omega}) + \sum_{i=1}^p \sum_{j=1}^p \text{SCAD}_{\lambda,a}(|\omega_{ij}|) \right\},$$

where the SCAD function $\text{SCAD}_{\lambda,a}$ is that proposed by Fan (1997). We use Fan and Li's (2001) recommended choice $a = 3.7$ throughout and set all λ to be the same for all (i, j) entries for simplicity. This setting for a and λ is the same as that of Fan, Feng, and Wu (2009). (See Fan, Feng, and Wu (2009) for further details on $\hat{\boldsymbol{\Omega}}_{\text{SCAD}}$.) Note that $\hat{\boldsymbol{\Omega}}_{\text{Glasso}}$ performs equivalently to the SPICE estimator of Rothman et al. (2008) according to their study.

We consider three models as follows:

- *Model 1.* $\omega_{ij}^0 = 0.6^{|i-j|}$.
- *Model 2.* The second model comes from Rothman et al. (2008). We let $\boldsymbol{\Omega}_0 = \mathbf{B} + \delta \mathbf{I}$, where each off-diagonal entry in \mathbf{B} is generated independently and equals 0.5 with probability 0.1 or 0 with probability 0.9. δ is chosen such

that the conditional number (the ratio of maximal and minimal singular values of a matrix) is equal to p . Finally, the matrix is standardized to have unit diagonals.

- *Model 3.* In this model, we consider a nonsparse matrix and let Ω_0 have all off-diagonal elements 0.5 and the diagonal elements 1.

Model 1 has a banded structure, and the values of the entries decay as they move away from the diagonal. Model 2 is an example of a sparse matrix without any special sparsity patterns. Model 3 serves as a dense matrix example.

For each model, we generate a training sample of size $n = 100$ from a multivariate normal distribution with mean 0 and covariance matrix Σ_0 , and an independent sample of size 100 from the same distribution for validating the tuning parameter λ . Using the training data, we compute a series of estimators with 50 different values of λ and use the one with the smallest likelihood loss on the validation sample, where the likelihood loss is defined by

$$L(\Sigma, \Omega) = \langle \Omega, \Sigma \rangle - \log \det(\Omega).$$

We compute the Glasso and SCAD estimators on the same training and testing data using the same cross-validation scheme. We consider different values of $p = 30, 60, 90, 120, 200$ and replicate 100 times.

We first measure the estimation quality by the following matrix norms: the operator norm, the matrix ℓ_1 norm, and the Frobenius norm. Table 1 reports the averages and standard errors of these losses.

We see that CLIME nearly uniformly outperforms Glasso. The improvement tends to be slightly more significant for sparse models when p is large, but overall the improvement is not dramatic. SCAD is the most computationally costly of the three methods, but numerically it has the best performance when $p < n$ and is comparable to CLIME when p is large. Note that SCAD uses a nonconvex penalty to correct the bias, whereas CLIME currently optimizes the convex ℓ_1 norm objective efficiently. A more comparable procedure that also corrects the bias is our two-stage Refitted CLIME, denoted by $\hat{\Omega}_{R-CLIME}$. Table 2 illustrates the improvement from bias correction, and we only list the spectral norm loss for reasons of space. It is clear that our Refitted CLIME estimator has comparable or better performance than SCAD, and our Refitted CLIME is especially favorable when p is large.

Gaussian graphical model selection has also received considerable attention in the literature. As we discussed earlier, this is equivalent to the support recovery of the precision matrix. The proportion of true zero (TN) and nonzero (TP) elements recovered by two methods are also reported here in Table 3. The numerical values over 10^{-3} in magnitude are considered to be nonzero, because the computation accuracy is set to be 10^{-4} .

It is noticeable that Glasso tends to be more noisy by including erroneous nonzero elements; CLIME tends to be more sparse than Glasso, which is usually favorable in real applications; SCAD produces the most sparse among the three but with a price of erroneously estimating more true nonzero entries by zero. This conclusion also can be reached in Figure 2, where the TPR and FPR values of 100 realizations of these three procedures for first two models (note that all elements in Model 3

are nonzero) are plotted for $p = 60$ as a representative example of other cases.

To better illustrate the recovery performance elementwise, Figure 3 shows heatmaps of the nonzeros identified out of 100 replications. All of the heatmaps suggest that CLIME is more sparse than Glasso, and visual inspection shows that the sparsity pattern recovered by CLIME has a significantly closer resemblance to the true model than Glasso. When the true model has significant nonzero elements scattered on the off-diagonals, Glasso tends to include more nonzero elements than are needed. SCAD is the sparsest of the three methods but again could zero out more true nonzero entries, as shown in Model 1. Similar patterns were observed in our experiments for other values of p .

5.2 Analysis of a Breast Cancer Dataset

We now apply our CLIME method on a real data example. The breast cancer data were analyzed by Hess et al. (2006) and are available at <http://bioinformatics.mdanderson.org/>. The dataset consists of 22,283 gene expression levels of 133 subjects, including 34 subjects with pathological complete response (pCR) and 99 subjects with residual disease (RD). The pCR subjects are considered to have a high chance of cancer-free survival in the long term, and thus it is of great interest to study the response states of the patients (pCR or RD) to neoadjuvant (preoperative) chemotherapy. Based on the estimated inverse covariance matrix of the gene expression levels, we apply linear discriminant analysis (LDA) to predict whether or not a subject can achieve the pCR state.

For a fair comparison with other methods of estimating the inverse covariance matrix, we follow the same analysis scheme used by Fan, Feng, and Wu (2009) and the references therein. For completeness, we briefly describe these steps here. The data are randomly divided into the training and testing datasets. A stratified sampling approach is applied to divide the data, with 5 pCR subjects and 16 RD subjects randomly selected to constitute the testing data (roughly 1/6 of the subjects in each group). The remaining subjects form the training set. For the training set, a two-sample t test is performed between the two groups for each gene, and the 113 most significant genes (i.e., with the smallest p -values) are retained as the covariates for prediction. Note that the size of the training sample is 112, 1 less than the variable size, which allows us to examine the performance when $p > n$. The gene data are then standardized by the estimated standard deviation, estimated from the training data. Finally, following the LDA framework, the normalized gene expression data are assumed to be normally distributed as $N(\mu_k, \Sigma)$, where the two groups are assumed to have the same covariance matrix, Σ , but different means, μ_k , $k = 1$ for pCR and $k = 2$ for RD. The estimated inverse covariance $\hat{\Omega}$ produced by different methods is used in the LDA scores,

$$\delta_k(\mathbf{x}) = \mathbf{x}^T \hat{\Omega} \hat{\mu}_k - \frac{1}{2} \hat{\mu}_k^T \hat{\Omega} \hat{\mu}_k + \log \hat{\pi}_k, \quad (20)$$

where $\hat{\pi}_k = n_k/n$ is the proportion of group k subjects in the training set and $\hat{\mu}_k = (1/n_k) \sum_{i \in \text{group } k} \mathbf{x}_i$ is the within-group average vector in the training set. The classification rule is taken to be $\hat{k}(\mathbf{x}) = \arg \max \delta_k(\mathbf{x})$ for $k = 1, 2$.

The classification performance is clearly associated with the estimation accuracy of $\hat{\Omega}$. We use the testing dataset to assess

Table 1. Comparison of average (SE) matrix losses for three models over 100 replications

p	Model 1			Model 2			Model 3		
	$\hat{\Omega}_{\text{CLIME}}$	$\hat{\Omega}_{\text{Glasso}}$	$\hat{\Omega}_{\text{SCAD}}$	$\hat{\Omega}_{\text{CLIME}}$	$\hat{\Omega}_{\text{Glasso}}$	$\hat{\Omega}_{\text{SCAD}}$	$\hat{\Omega}_{\text{CLIME}}$	$\hat{\Omega}_{\text{Glasso}}$	$\hat{\Omega}_{\text{SCAD}}$
	Operator norm								
30	2.28 (0.02)	2.48 (0.01)	2.38 (0.02)	0.74 (0.01)	0.77 (0.01)	0.59 (0.02)	14.95 (0.004)	14.96 (0.004)	14.97 (0.002)
60	2.79 (0.01)	2.93 (0.01)	2.71 (0.01)	1.13 (0.01)	1.12 (0.01)	0.95 (0.01)	30.01 (0.002)	30.02 (0.002)	29.98 (0.001)
90	2.97 (0.01)	3.07 (0.004)	2.76 (0.004)	1.69 (0.01)	1.49 (0.004)	1.14 (0.01)	45.01 (0.002)	45.03 (0.001)	44.98 (0.001)
120	3.08 (0.004)	3.14 (0.003)	2.79 (0.004)	2.16 (0.01)	1.82 (0.003)	1.38 (0.01)	60.01 (0.002)	60.04 (0.001)	58.40 (0.10)
200	3.17 (0.01)	3.25 (0.002)	2.83 (0.003)	2.36 (0.01)	2.46 (0.002)	2.11 (0.01)	100.02 (0.001)	100.08 (0.001)	96.69 (0.01)
	Matrix ℓ_1 -norm								
30	2.91 (0.02)	3.08 (0.01)	2.91 (0.02)	1.29 (0.02)	1.36 (0.01)	0.81 (0.02)	15.12 (0.004)	15.08 (0.003)	15.10 (0.002)
60	3.32 (0.01)	3.55 (0.01)	3.11 (0.01)	2.10 (0.02)	2.11 (0.02)	1.98 (0.03)	30.17 (0.002)	30.15 (0.002)	30.12 (0.002)
90	3.44 (0.01)	3.72 (0.01)	3.19 (0.01)	2.95 (0.02)	2.87 (0.02)	2.71 (0.03)	45.18 (0.002)	45.18 (0.002)	45.13 (0.002)
120	3.48 (0.01)	3.81 (0.01)	3.24 (0.01)	3.69 (0.02)	3.33 (0.02)	3.32 (0.03)	60.20 (0.002)	60.20 (0.003)	60.55 (0.06)
200	3.55 (0.01)	4.01 (0.01)	3.37 (0.01)	4.13 (0.02)	4.52 (0.02)	4.67 (0.03)	100.22 (0.002)	100.24 (0.002)	102.64 (0.05)
	Frobenius norm								
30	3.81 (0.04)	4.23 (0.03)	3.97 (0.03)	1.72 (0.02)	1.71 (0.01)	1.23 (0.02)	14.96 (0.004)	14.97 (0.004)	14.97 (0.001)
60	6.63 (0.03)	7.14 (0.02)	6.37 (0.02)	3.33 (0.02)	3.10 (0.01)	3.11 (0.01)	30.02 (0.002)	30.02 (0.002)	29.98 (0.001)
90	8.78 (0.04)	9.25 (0.01)	7.98 (0.01)	4.92 (0.02)	4.36 (0.01)	4.51 (0.01)	45.02 (0.002)	45.04 (0.001)	44.99 (0.001)
120	10.58 (0.02)	10.97 (0.01)	9.31 (0.01)	6.50 (0.03)	5.50 (0.01)	5.89 (0.01)	60.01 (0.001)	60.05 (0.001)	60.60 (0.08)
200	14.20 (0.04)	14.85 (0.01)	12.21 (0.01)	7.57 (0.02)	8.15 (0.01)	8.41 (0.01)	100.02 (0.001)	100.08 (0.001)	103.41 (0.02)

Table 2. Comparison of average (SE) operator norm losses from Models 1 and 2 over 100 replications

p	Model 1		Model 2	
	$\hat{\Omega}_{R-CLIME}$	$\hat{\Omega}_{SCAD}$	$\hat{\Omega}_{R-CLIME}$	$\hat{\Omega}_{SCAD}$
30	1.56 (0.02)	2.38 (0.02)	0.85 (0.01)	0.59 (0.02)
60	2.15 (0.01)	2.71 (0.01)	1.14 (0.01)	0.95 (0.09)
90	2.42 (0.01)	2.76 (0.004)	1.17 (0.01)	1.14 (0.01)
120	2.56 (0.01)	2.79 (0.004)	1.44 (0.01)	1.38 (0.01)
200	2.71 (0.01)	2.83 (0.003)	1.91 (0.01)	2.11 (0.01)

the estimation performance and to make comparisons with the existing results of Fan, Feng, and Wu (2009) using the same criterion. For the tuning parameters, we use a 6-fold cross-validation on the training data for choosing λ . We repeat the foregoing estimation scheme 100 times.

To compare the classification performance, we use specificity, sensitivity, and Mathews correlation coefficient (MCC) criteria, defined as follows:

$$\text{Specificity} = \frac{TN}{TN + FP}, \quad \text{Sensitivity} = \frac{TP}{TP + FN},$$

$$\text{MCC} = \frac{TP \times TN - FP \times FN}{\sqrt{(TP + FP)(TP + FN)(TN + FP)(TN + FN)}}.$$

Here TP and TN stand for true positives (pCR) and true negatives (RD), respectively, and FP and FN stand for false positives/negatives. The larger the criterion value, the better the classification performance. The averages and standard errors of the foregoing criteria, along with the number of nonzero entries in $\hat{\Omega}$ over 100 replications, are reported in Table 4. The Glasso, Adaptive lasso, and SCAD results are taken from the work of Fan, Feng, and Wu (2009), which used the same procedure on the same data set, except that here we use $\hat{\Omega}_{CLIME}$ in place of $\hat{\Omega}$.

Clearly, CLIME significantly outperforms the other two methods on sensitivity and is comparable with them on specificity. The overall classification performance measured by MCC overwhelmingly favors CLIME, which shows a 25% improvement over the best alternative methods. CLIME also produces the sparsest matrix, which is usually favorable for interpretation purposes on real datasets.

6. DISCUSSION

This article presents a new constrained ℓ_1 minimization method for estimating high-dimensional precision matrices. Both the method and the analysis are relatively simple and straightforward, and may be extended to other related problems. Moreover, the method and the results are not restricted to a specific sparsity pattern. Thus the estimator can be used to recover a wide class of matrices in theory as well as in applications. In particular, when applying our method to covariance selection in Gaussian graphical models, the theoretical results can be established without assuming the irrepresentable condition of Ravikumar et al. (2008), which is very stringent and hard to check in practice.

Several authors, including Yuan and Lin (2007), Rothman et al. (2008), and Ravikumar et al. (2008), have estimated the precision matrix by solving the optimization problem (16) with ℓ_1

penalty only on the off-diagonal entries, which is slightly different from our starting point (4) presented here. We also can consider the following optimization problem:

$$\min \|\Omega\|_{1,\text{off}} \quad \text{subject to: } |\Sigma_n \Omega - \mathbf{I}|_\infty \leq \lambda_n, \quad \Omega \in \mathbb{R}^{p \times p}.$$

Analogous results can be established for the foregoing estimator. We omit these here, due to close resemblance in proof techniques and conclusions.

There are several possible extensions of our method. For example, Zhou, Lafferty, and Wasserman (2010) considered the time-varying undirected graphs and estimated $\Sigma(t)^{-1}$ by Glasso. It would be very interesting to study the estimation of $\Sigma(t)^{-1}$ by our method. Ravikumar and Wainwright (2009) considered high-dimensional Ising model selection using ℓ_1 -regularized logistic regression. It would be interesting to apply our method to their setting as well.

Another important subject is investigating the theoretical property of the tuning parameter selected by the cross-validation method, although based on our experiments, CLIME is not very sensitive to the choice of tuning parameter. An example of such results on cross-validation was provided by Bickel and Levina (2008b) on thresholding.

After submitting this article for publication, we were made aware that Zhang (2010) had proposed a precision matrix estimator, called GMACS, which is the solution of the following optimization problem:

$$\min \|\Omega\|_{L_1} \quad \text{subject to: } |\Sigma_n \Omega - \mathbf{I}|_\infty \leq \lambda_n, \quad \Omega \in \mathbb{R}^{p \times p}.$$

The objective function here is different from that of CLIME, and this basic version cannot be solved column-by-column and is not as easy to implement. Zhang (2010) considered only the Gaussian case and ℓ_0 balls, whereas we consider sub-Gaussian and polynomial-tail distributions and more general ℓ_q balls. In addition, the GMACS estimator requires an additional thresholding step for the rates to hold over ℓ_0 balls. In contrast, CLIME does not need an additional thresholding step, and the rates hold over general ℓ_q balls.

7. PROOF OF MAIN RESULTS

Proof of Lemma 1. Write $\Omega = (\omega_1, \dots, \omega_p)$, where $\omega_i \in \mathbb{R}^p$. The constraint $|\Sigma_n \Omega - \mathbf{I}|_\infty \leq \lambda_n$ is equivalent to

$$|\Sigma_n \omega_i - \mathbf{e}_i|_\infty \leq \lambda_n \quad \text{for } 1 \leq i \leq p.$$

Thus we have

$$|\hat{\omega}_i^1|_1 \geq |\hat{\beta}_i|_1 \quad \text{for } 1 \leq i \leq p. \tag{21}$$

Because $|\Sigma_n \hat{\mathbf{B}} - \mathbf{I}|_\infty \leq \lambda_n$, by the definitions of $\{\hat{\Omega}_1\}$, we have

$$\|\hat{\Omega}_1\|_1 \leq \|\hat{\mathbf{B}}\|_1. \tag{22}$$

By (21) and (22), we have $\hat{\mathbf{B}} \in \{\hat{\Omega}_1\}$. On the other hand, if $\hat{\Omega}_1 \notin \{\hat{\mathbf{B}}\}$, then there exists an i such that $|\hat{\omega}_i|_1 > |\hat{\beta}_i|_1$. Thus, by (21), we have $\|\hat{\Omega}_1\|_1 > \|\hat{\mathbf{B}}\|_1$. This is in conflict with (22).

The main results all rely on Theorem 6, which upper bounds the elementwise ℓ_∞ norm. We prove this theorem first.

Proof of Theorem 6. Let $\hat{\beta}_{i,\rho}$ be a solution of (3) by replacing Σ_n with $\Sigma_{n,\rho}$. Note that Lemma 1 still holds for $\hat{\Omega}_{n,\rho}$ and $\{\hat{\beta}_{i,\rho}\}$ with $\rho \geq 0$. For conciseness of notation, we only prove the theorem for $\rho = 0$. The proof is exactly the same for general

Table 3. Comparison of average (SE) support recovery for three models over 100 replications

p	Model 1			Model 2			Model 3		
	$\hat{\Omega}_{\text{CLIME}}$	$\hat{\Omega}_{\text{Glasso}}$	$\hat{\Omega}_{\text{SCAD}}$	$\hat{\Omega}_{\text{CLIME}}$	$\hat{\Omega}_{\text{Glasso}}$	$\hat{\Omega}_{\text{SCAD}}$	$\hat{\Omega}_{\text{CLIME}}$	$\hat{\Omega}_{\text{Glasso}}$	$\hat{\Omega}_{\text{SCAD}}$
					TN%				
30	78.69 (0.61)	50.65 (0.75)	99.26 (0.17)	77.41 (0.86)	64.70 (0.42)	99.10 (0.08)	N/A	N/A	N/A
60	90.37 (0.27)	69.47 (0.29)	99.86 (0.03)	85.98 (0.36)	69.44 (0.21)	96.08 (0.14)	N/A	N/A	N/A
90	94.30 (0.27)	77.62 (0.20)	99.88 (0.02)	91.15 (0.17)	71.57 (0.15)	95.98 (0.11)	N/A	N/A	N/A
120	96.45 (0.06)	81.46 (0.16)	99.91 (0.01)	94.87 (0.19)	75.33 (0.10)	95.69 (0.10)	N/A	N/A	N/A
200	97.41 (0.11)	85.36 (0.11)	99.92 (0.01)	81.74 (0.26)	66.07 (0.12)	96.97 (0.05)	N/A	N/A	N/A
					TP%				
30	41.07 (0.58)	60.20 (0.56)	16.93 (0.28)	99.66 (0.09)	99.98 (0.02)	97.70 (0.24)	14.88 (0.50)	20.07 (0.57)	3.38 (0.001)
60	25.96 (0.30)	41.72 (0.32)	12.72 (0.15)	85.10 (0.36)	96.47 (0.13)	79.81 (0.44)	6.86 (0.05)	10.49 (0.20)	1.67 (0.001)
90	20.32 (0.32)	33.70 (0.23)	11.94 (0.09)	66.25 (0.39)	91.62 (0.15)	67.93 (0.48)	5.86 (0.03)	7.54 (0.13)	1.11 (0.001)
120	17.16 (0.09)	29.32 (0.20)	11.57 (0.07)	42.37 (0.49)	82.45 (0.15)	54.92 (0.41)	5.11 (0.02)	6.20 (0.12)	20.63 (2.47)
200	15.03 (0.13)	25.34 (0.15)	11.07 (0.06)	57.07 (0.27)	73.43 (0.14)	30.50 (0.40)	3.56 (0.01)	4.94 (0.02)	39.76 (0.02)

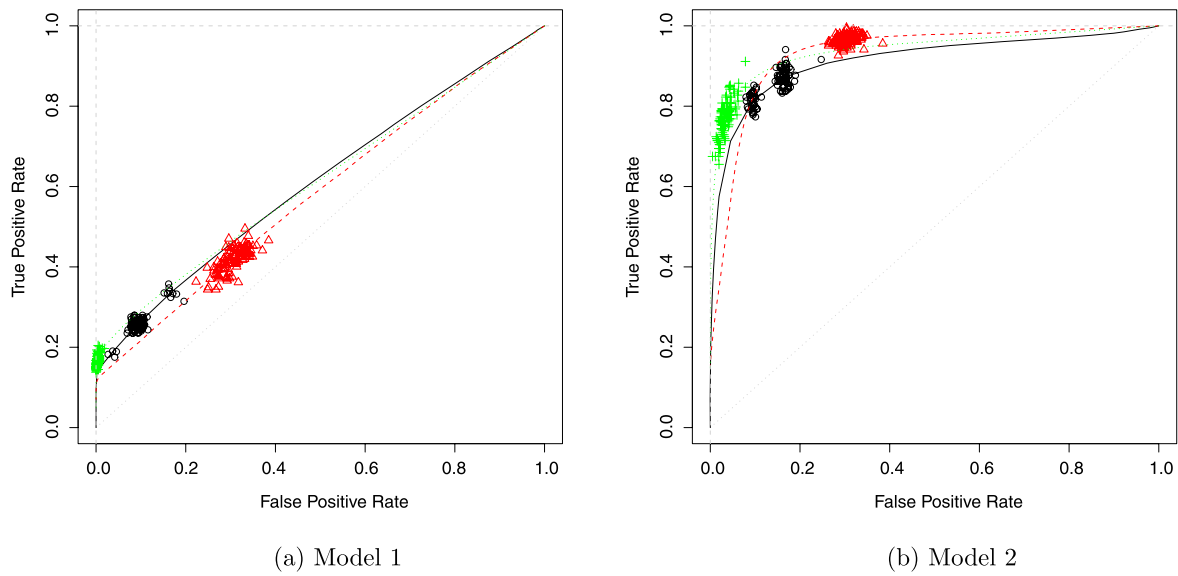


Figure 2. TPR vs FPR for $p = 60$. The solid, dashed and dotted lines are the average TPR and FPR values for CLIME, Glasso, and SCAD, respectively, as the tuning parameters of these methods vary. The circles, triangles and pluses correspond to 100 different realizations of CLIME, Glasso and SCAD respectively, with the tuning parameter picked by cross validation.

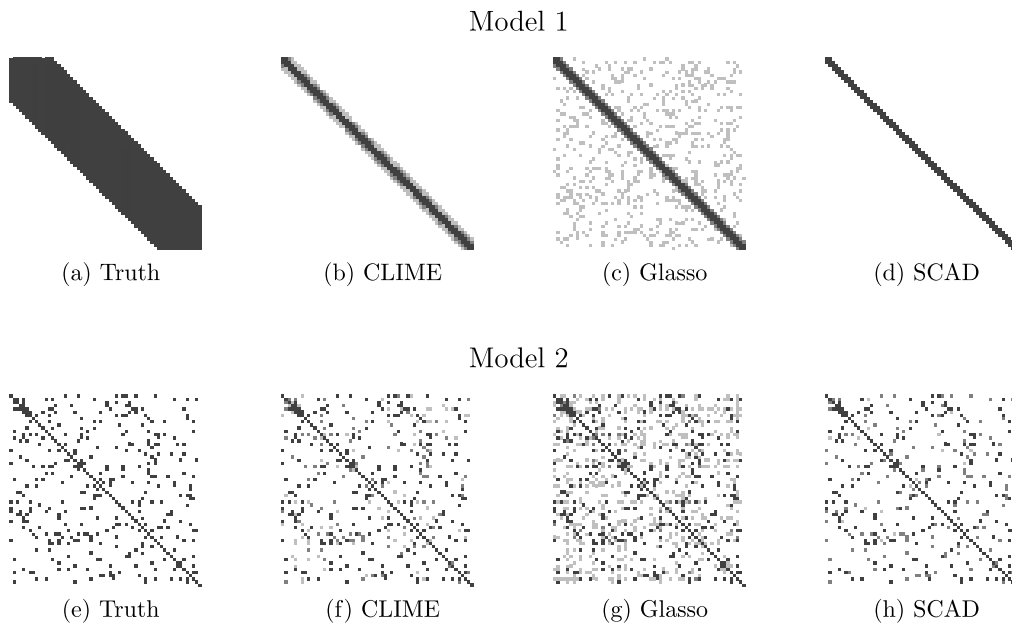


Figure 3. Heatmaps of the frequency of the zeros identified for each entry of the precision matrix (when $p = 60$) out of 100 replications. White represents 100 zeros identified out of 100 runs, and black represents 0/100.

Table 4. Comparison of average (SE) pCR classification errors over 100 replications. Glasso, Adaptive lasso, and SCAD results are taken from Fan, Feng, and Wu (2009, table 2)

Method	Specificity	Sensitivity	MCC	Nonzero entries in $\hat{\Omega}$
Glasso	0.768 (0.009)	0.630 (0.021)	0.366 (0.018)	3923 (2)
Adaptive lasso	0.787 (0.009)	0.622 (0.022)	0.381 (0.018)	1233 (1)
SCAD	0.794 (0.009)	0.634 (0.022)	0.402 (0.020)	674 (1)
CLIME	0.749 (0.005)	0.806 (0.017)	0.506 (0.020)	492 (7)

$\rho > 0$. By the condition in Theorem 6,

$$|\boldsymbol{\Sigma}_0 - \boldsymbol{\Sigma}_n|_\infty \leq \lambda_n / \|\boldsymbol{\Omega}_0\|_{L_1}. \quad (23)$$

We then have

$$\begin{aligned} |\mathbf{I} - \boldsymbol{\Sigma}_n \boldsymbol{\Omega}_0|_\infty &= |(\boldsymbol{\Sigma}_0 - \boldsymbol{\Sigma}_n) \boldsymbol{\Omega}_0|_\infty \\ &\leq \|\boldsymbol{\Omega}_0\|_{L_1} |\boldsymbol{\Sigma}_0 - \boldsymbol{\Sigma}_n|_\infty \leq \lambda_n, \end{aligned} \quad (24)$$

where we use the inequality $|\mathbf{A}\mathbf{B}|_\infty \leq |\mathbf{A}|_\infty \|\mathbf{B}\|_{L_1}$ for matrices \mathbf{A}, \mathbf{B} of appropriate sizes. By the definition of $\hat{\boldsymbol{\beta}}_i$, we can see that $|\hat{\boldsymbol{\beta}}_i|_1 \leq \|\boldsymbol{\Omega}_0\|_{L_1}$ for $1 \leq i \leq p$. By Lemma 1,

$$\|\hat{\boldsymbol{\Omega}}_1\|_{L_1} \leq \|\boldsymbol{\Omega}_0\|_{L_1}. \quad (25)$$

We have

$$\begin{aligned} |\boldsymbol{\Sigma}_n(\hat{\boldsymbol{\Omega}}_1 - \boldsymbol{\Omega}_0)|_\infty &\leq |\boldsymbol{\Sigma}_n \hat{\boldsymbol{\Omega}}_1 - \mathbf{I}|_\infty + |\mathbf{I} - \boldsymbol{\Sigma}_n \boldsymbol{\Omega}_0|_\infty \\ &\leq 2\lambda_n. \end{aligned} \quad (26)$$

Therefore, by (23)–(26),

$$\begin{aligned} |\boldsymbol{\Sigma}_0(\hat{\boldsymbol{\Omega}}_1 - \boldsymbol{\Omega}_0)|_\infty &\leq |\boldsymbol{\Sigma}_n(\hat{\boldsymbol{\Omega}}_1 - \boldsymbol{\Omega}_0)|_\infty + |(\boldsymbol{\Sigma}_n - \boldsymbol{\Sigma}_0)(\hat{\boldsymbol{\Omega}}_1 - \boldsymbol{\Omega}_0)|_\infty \\ &\leq 2\lambda_n + \|\hat{\boldsymbol{\Omega}}_1 - \boldsymbol{\Omega}_0\|_{L_1} |\boldsymbol{\Sigma}_n - \boldsymbol{\Sigma}_0|_\infty \leq 4\lambda_n. \end{aligned}$$

It follows that

$$|\hat{\boldsymbol{\Omega}}_1 - \boldsymbol{\Omega}_0|_\infty \leq \|\boldsymbol{\Omega}_0\|_{L_1} |\boldsymbol{\Sigma}_0(\hat{\boldsymbol{\Omega}}_1 - \boldsymbol{\Omega}_0)|_\infty \leq 4\|\boldsymbol{\Omega}_0\|_{L_1} \lambda_n.$$

This establishes (13) by the definition in (2).

We next prove (14). Let $t_n = |\hat{\boldsymbol{\Omega}} - \boldsymbol{\Omega}_0|_\infty$ and define

$$\mathbf{h}_j = \hat{\boldsymbol{\omega}}_j - \boldsymbol{\omega}_j^0,$$

$$\mathbf{h}_j^1 = (\hat{\boldsymbol{\omega}}_{ij} I\{\hat{\boldsymbol{\omega}}_{ij} \geq 2t_n\}; 1 \leq i \leq p)^T - \boldsymbol{\omega}_j^0, \quad \mathbf{h}_j^2 = \mathbf{h}_j - \mathbf{h}_j^1.$$

By the definition (2) of $\hat{\boldsymbol{\Omega}}$, we have $|\hat{\boldsymbol{\omega}}_j|_1 \leq |\hat{\boldsymbol{\omega}}_j^1|_1 \leq |\boldsymbol{\omega}_j^0|_1$. Then

$$|\boldsymbol{\omega}_j^0|_1 - |\mathbf{h}_j^1|_1 + |\mathbf{h}_j^2|_1 \leq |\boldsymbol{\omega}_j^0|_1 + |\mathbf{h}_j^1|_1 + |\mathbf{h}_j^2|_1 = |\hat{\boldsymbol{\omega}}_j|_1 \leq |\boldsymbol{\omega}_j^0|_1,$$

which implies that $|\mathbf{h}_j^2|_1 \leq |\mathbf{h}_j^1|_1$. It follows that $|\mathbf{h}_j|_1 \leq 2|\mathbf{h}_j^1|_1$.

Thus we only need to upper bound $|\mathbf{h}_j^1|_1$. We have

$$\begin{aligned} |\mathbf{h}_j^1|_1 &= \sum_{i=1}^p |\hat{\boldsymbol{\omega}}_{ij} I\{\hat{\boldsymbol{\omega}}_{ij} \geq 2t_n\} - \omega_{ij}^0| \\ &\leq \sum_{i=1}^p |\omega_{ij}^0 I\{\omega_{ij}^0 \leq 2t_n\}| \\ &\quad + \sum_{i=1}^p |\hat{\boldsymbol{\omega}}_{ij} I\{\hat{\boldsymbol{\omega}}_{ij} \geq 2t_n\} - \omega_{ij}^0 I\{\omega_{ij}^0 \geq 2t_n\}| \\ &\leq (2t_n)^{1-q} s_0(p) + t_n \sum_{i=1}^p I\{\hat{\boldsymbol{\omega}}_{ij} \geq 2t_n\} \\ &\quad + \sum_{i=1}^p |\omega_{ij}^0| |I\{\hat{\boldsymbol{\omega}}_{ij} \geq 2t_n\} - I\{\omega_{ij}^0 \geq 2t_n\}| \\ &\leq (2t_n)^{1-q} s_0(p) + t_n \sum_{i=1}^p I\{\omega_{ij}^0 \geq t_n\} \\ &\quad + \sum_{i=1}^p |\omega_{ij}^0| |I\{|\omega_{ij}^0| - 2t_n \leq \hat{\boldsymbol{\omega}}_{ij} - \omega_{ij}^0\}| \end{aligned}$$

$$\begin{aligned} &\leq (2t_n)^{1-q} s_0(p) + (t_n)^{1-q} s_0(p) + (3t_n)^{1-q} s_0(p) \\ &\leq (1 + 2^{1-q} + 3^{1-q}) t_n^{1-q} s_0(p), \end{aligned} \quad (27)$$

where we use the following inequality: for any $a, b, c \in \mathbb{R}$, we have

$$|I\{a < c\} - I\{b < c\}| \leq I\{|b - c| < |a - b|\}.$$

This completes the proof of (14).

Finally, (15) follows from (13), (27), and the inequality $\|\mathbf{A}\|_F^2 \leq p \|\mathbf{A}\|_{L_1} \|\mathbf{A}\|_\infty$ for any $p \times p$ matrix.

Proof of Theorems 1(a) and 4(a). By Theorem 6, we only need to prove

$$\max_{ij} |\hat{\sigma}_{ij} - \sigma_{ij}^0| \leq C_0 \sqrt{\log p / n} \quad (28)$$

with probability greater than $1 - 4p^{-\tau}$ under (C1). Without loss of generality, we assume that $\mathbf{E}\mathbf{X} = 0$. Let $\boldsymbol{\Sigma}_n^0 := n^{-1} \sum_{k=1}^n \mathbf{X}_k \mathbf{X}_k^T$ and $Y_{kij} = X_{ki} X_{kj} - \mathbf{E}X_{ki} X_{kj}$. We then have $\boldsymbol{\Sigma}_n = \boldsymbol{\Sigma}_n^0 - \bar{\mathbf{X}} \bar{\mathbf{X}}^T$. Let $t = \eta \sqrt{\log p / n}$. Using the inequality $|e^s - 1 - s| \leq s^2 e^{\max(s, 0)}$ for any $s \in \mathbb{R}$ and letting $C_{K1} = 2 + \tau + \eta^{-1} K^2$, by basic calculations, we can get

$$\begin{aligned} &\mathbf{P}\left(\sum_{k=1}^n Y_{kij} \geq \eta^{-1} C_{K1} \sqrt{n \log p}\right) \\ &\leq e^{-C_{K1} \log p} (\mathbf{E} \exp(t Y_{kij}))^n \\ &\leq \exp(-C_{K1} \log p + n t^2 \mathbf{E} Y_{kij}^2 e^{t|Y_{kij}|}) \\ &\leq \exp(-C_{K1} \log p + \eta^{-1} K^2 \log p) \\ &\leq \exp(-(\tau + 2) \log p). \end{aligned}$$

Thus, we have

$$\mathbf{P}(|\boldsymbol{\Sigma}_n^0 - \boldsymbol{\Sigma}_0|_\infty \geq \eta^{-1} C_{K1} \sqrt{\log p / n}) \leq 2p^{-\tau}. \quad (29)$$

By the simple inequality $e^s \leq e^{s^2+1}$ for $s > 0$, we have $\mathbf{E}e^{t|X_{ki}|} \leq eK$ for all $t \leq \eta^{1/2}$. Let $C_{K2} = 2 + \tau + \eta^{-1} e^2 K^2$ and $a_n = C_{K2}^2 (\log p / n)^{1/2}$. As before, we can show that

$$\begin{aligned} &\mathbf{P}(|\bar{\mathbf{X}} \bar{\mathbf{X}}^T|_\infty \geq \eta^{-2} a_n \sqrt{\log p / n}) \\ &\leq p \max_i \mathbf{P}\left(\sum_{k=1}^n X_{ki} \geq \eta^{-1} C_{K2} \sqrt{n \log p}\right) \\ &\quad + p \max_i \mathbf{P}\left(-\sum_{k=1}^n X_{ki} \geq \eta^{-1} C_{K2} \sqrt{n \log p}\right) \\ &\leq 2p^{-\tau-1}. \end{aligned} \quad (30)$$

By (29), (30), and the inequality $C_0 > \eta^{-1} C_{K1} + \eta^{-2} a_n$, we see that (28) holds.

Proof of Theorems 1(b) and 4(b). Let

$$\begin{aligned} \bar{Y}_{kij} &= X_{ki} X_{kj} I\{|X_{ki} X_{kj}| \leq \sqrt{n / (\log p)^3}\} \\ &\quad - \mathbf{E}X_{ki} X_{kj} I\{|X_{ki} X_{kj}| \leq \sqrt{n / (\log p)^3}\}, \\ \check{Y}_{kij} &= Y_{kij} - \bar{Y}_{kij}. \end{aligned}$$

Because $b_n := \max_{i,j} \mathbb{E}|X_{ki}X_{kj}|I\{|X_{ki}X_{kj}| \geq \sqrt{n/(\log p)^3}\} = O(1)n^{-\nu-1/2}$, we have, by (C2),

$$\begin{aligned} & \mathbb{P}\left(\max_{i,j} \left| \sum_{k=1}^n \check{Y}_{kij} \right| \geq 2nb_n\right) \\ & \leq \mathbb{P}\left(\max_{i,j} \left| \sum_{k=1}^n X_{ki}X_{kj}I\{|X_{ki}X_{kj}| > \sqrt{n/(\log p)^3}\} \right| \geq nb_n\right) \\ & \leq \mathbb{P}\left(\max_{i,j} \sum_{k=1}^n |X_{ki}X_{kj}|I\{X_{ki}^2 + X_{kj}^2 \geq 2\sqrt{n/(\log p)^3}\} \geq nb_n\right) \\ & \leq \mathbb{P}\left(\max_{k,i} X_{ki}^2 \geq \sqrt{n/(\log p)^3}\right) \\ & \leq pn\mathbb{P}(X_1^2 \geq \sqrt{n/(\log p)^3}) \\ & = O(1)n^{-\delta/8}. \end{aligned}$$

By Bernstein’s inequality (cf. Bennett 1962) and some elementary calculations,

$$\begin{aligned} & \mathbb{P}\left(\max_{i,j} \left| \sum_{k=1}^n \bar{Y}_{kij} \right| \geq \sqrt{(\theta + 1)(4 + \tau)n \log p}\right) \\ & \leq p^2 \max_{i,j} \mathbb{P}\left(\left| \sum_{k=1}^n \bar{Y}_{kij} \right| \geq \sqrt{(\theta + 1)(4 + \tau)n \log p}\right) \\ & \leq 2p^2 \max_{i,j} \exp(-(\theta + 1)(4 + \tau)n \log p \\ & \quad / (2n\mathbb{E}\bar{Y}_{ij}^2 + \sqrt{(\theta + 1)(64 + 16\tau)n/(3 \log p)})) \\ & = O(1)p^{-\tau/2}. \end{aligned}$$

Thus we have

$$\begin{aligned} \mathbb{P}(|\Sigma_n^0 - \Sigma_0|_\infty \geq \sqrt{(\theta + 1)(4 + \tau) \log p/n} + 2b_n) \\ = O(n^{-\delta/8} + p^{-\tau/2}). \end{aligned} \tag{31}$$

Using the same truncation argument and Bernstein’s inequality, we can show that

$$\begin{aligned} \mathbb{P}\left(\max_i \left| \sum_{k=1}^n X_{ki} \right| \geq \sqrt{\max_i \sigma_{ii}^0(4 + \tau)n \log p}\right) \\ = O(n^{-\delta/8} + p^{-\tau/2}). \end{aligned}$$

Thus

$$\begin{aligned} \mathbb{P}(|\bar{X}\bar{X}^T|_\infty \geq \max_i \sigma_{ii}^0(4 + \tau) \log p/n) \\ = O(n^{-\delta/8} + p^{-\tau/2}). \end{aligned} \tag{32}$$

Combining (31) and (32), we have

$$\max_{ij} |\hat{\sigma}_{ij} - \sigma_{ij}^0| \leq \sqrt{(\theta + 1)(5 + \tau) \log p/n} \tag{33}$$

with probability greater than $1 - O(n^{-\delta/8} + p^{-\tau/2})$. The proof is completed by (33) and Theorem 6.

Proof of Theorems 2 and 5. Because $\Sigma_{n,\rho}^{-1}$ is a feasible point, we have, by (10),

$$\|\hat{\Omega}_\rho\|_1 \leq \|\hat{\Omega}_{1,\rho}\|_1 \leq \|\Sigma_{n,\rho}^{-1}\|_1 \leq p^2 \max\left(\sqrt{\frac{n}{\log p}}, p^\alpha\right).$$

By (28), Theorem 6, the fact $p \geq n^\xi$, and because τ is large enough, we have

$$\begin{aligned} \sup_{\Omega_0 \in \mathcal{U}} \mathbb{E}\|\hat{\Omega}_\rho - \Omega_0\|_2^2 &= \sup_{\Omega_0 \in \mathcal{U}} \mathbb{E}\|\hat{\Omega}_\rho - \Omega_0\|_2^2 \\ &\quad \times I\left\{\max_{ij} |\hat{\sigma}_{ij} - \sigma_{ij}^0| + \rho \leq C_0\sqrt{\log p/n}\right\} \\ &\quad + \sup_{\Omega_0 \in \mathcal{U}} \mathbb{E}\|\hat{\Omega}_\rho - \Omega_0\|_2^2 \\ &\quad \times I\left\{\max_{ij} |\hat{\sigma}_{ij} - \sigma_{ij}^0| + \rho > C_0\sqrt{\log p/n}\right\} \\ &= O\left(M^{4-4q} s_0^2(p) \left(\frac{\log p}{n}\right)^{1-q}\right) \\ &\quad + O\left(p^4 \max\left(\frac{n}{\log p}, p^{2\alpha}\right) p^{-\tau/2}\right) \\ &= O\left(M^{4-4q} s_0^2(p) \left(\frac{\log p}{n}\right)^{1-q}\right). \end{aligned}$$

This proves Theorem 2. The proof of Theorem 5 is similar.

Proof of Theorem 3. Let k_n be an integer satisfying $1 \leq k_n \leq n$. Define

$$\begin{aligned} \mathbf{h}_j &= \hat{\omega}_j - \omega_j^0, \\ \mathbf{h}_j^1 &= (\hat{\omega}_{ij}I\{1 \leq i \leq k_n\}; 1 \leq i \leq p)^T - \omega_j^0, \quad \mathbf{h}_j^2 = \mathbf{h}_j - \mathbf{h}_j^1. \end{aligned}$$

By the proof of Theorem 6, we can show that $|\mathbf{h}_j|_1 \leq 2|\mathbf{h}_j^1|_1$. Because $\Omega_0 \in \mathcal{U}_o(\alpha, M)$, we have $\sum_{j \geq k_n} |\omega_{ij}^0| \leq Mk_n^{-\alpha}$. By Theorem 4, $\sum_{j=1}^{k_n} |\hat{\omega}_{ij} - \omega_{ij}^0| = O(k_n\sqrt{\log p/n})$ with probability greater than $1 - O(n^{-\delta/8} + p^{-\tau/2})$. Theorem 3(a) is proved by taking $k_n = \lceil (n/\log p)^{1/(2\alpha+2)} \rceil$. The proof of Theorem 3(b) is similar as that of Theorem 2.

[Received March 2010. Revised January 2011.]

REFERENCES

Banerjee, O., Ghaoui, L. E., and d’Aspremont, A. (2008), “Model Selection Through Sparse Maximum Likelihood Estimation,” *Journal of Machine Learning Research*, 9, 485–516. [596]

Bennett, G. (1962), “Probability Inequalities for the Sum of Independent Random Variables,” *Journal of the American Statistical Association*, 57, 33–45. [606]

Bickel, P., and Levina, E. (2008a), “Regularized Estimation of Large Covariance Matrices,” *The Annals of Statistics*, 36, 199–227. [594,597]

——— (2008b), “Covariance Regularization by Thresholding,” *The Annals of Statistics*, 36, 2577–2604. [594,596,602]

Boyd, S., and Vandenberghe, L. (2004), *Convex Optimization*, Cambridge, U.K.: Cambridge University Press. [599]

Cai, T., Wang, L., and Xu, G. (2010), “Shifting Inequality and Recovery of Sparse Signals,” *IEEE Transactions on Signal Processing*, 58, 1300–1308. [595]

Cai, T., Zhang, C.-H., and Zhou, H. (2010), “Optimal Rates of Convergence for Covariance Matrix Estimation,” *The Annals of Statistics*, 38, 2118–2144. [594]

Candès, E., and Tao, T. (2007), “The Dantzig Selector, Statistical Estimation When p Is Much Larger Than n ,” *The Annals of Statistics*, 35, 2313–2351. [595,599]

d’Aspremont, A., Banerjee, O., and El Ghaoui, L. (2008), “First-Order Methods for Sparse Covariance Selection,” *SIAM Journal on Matrix Analysis and Its Applications*, 30, 56–66. [594,596]

Donoho, D., Elad, M., and Temlyakov, V. (2006), “Stable Recovery of Sparse Overcomplete Representations in the Presence of Noise,” *IEEE Transactions on Information Theory*, 52, 6–18. [595]

El Karoui, N. (2008), “Operator Norm Consistent Estimation of Large-Dimensional Sparse Covariance Matrices,” *The Annals of Statistics*, 36, 2717–2756. [594]

- Fan, J. (1997), Comment on “Wavelets in Statistics: A Review,” by A. Antoniadis, *Journal of the Italian Statistical Association*, 6, 131–138. [599]
- Fan, J., and Li, R. (2001), “Variable Selection via Nonconcave Penalized Likelihood and Its Oracle Properties,” *Journal of the American Statistical Association*, 96, 1348–1360. [599]
- Fan, J., Feng, Y., and Wu, Y. (2009), “Network Exploration via the Adaptive Lasso and SCAD Penalties,” *The Annals of Applied Statistics*, 2, 521–541. [594,599,600,602,604]
- Friedman, J., Hastie, T., and Tibshirani, R. (2008), “Sparse Inverse Covariance Estimation With the Graphical Lasso,” *Biostatistics*, 9, 432–441. [594,596]
- Hess, K. R., Anderson, K., Symmans, W. F., Valero, V., Ibrahim, N., Mejia, J. A., Booser, D., Theriault, R. L., Buzdar, A. U., Dempsey, P. J., Rouzier, R., Sneige, N., Ross, J. S., Vidaurre, T., Gómez, H. L., Hortobagyi, G. N., and Puztai, L. (2006), “Pharmacogenomic Predictor of Sensitivity to Preoperative Chemotherapy With Paclitaxel and Fluorouracil, Doxorubicin, and Cyclophosphamide in Breast Cancer,” *Journal of Clinical Oncology*, 24, 4236–4244. [600]
- Huang, J., Liu, N., Pourahmadi, M., and Liu, L. (2006), “Covariance Matrix Selection and Estimation via Penalized Normal Likelihood,” *Biometrika*, 93, 85–98. [594]
- Lam, C., and Fan, J. (2009), “Sparsistency and Rates of Convergence in Large Covariance Matrix Estimation,” *The Annals of Statistics*, 37, 4254–4278. [594,597]
- Lauritzen, S. L. (1996), *Graphical Models. Oxford Statistical Science Series*, New York: Oxford University Press. [595]
- Liu, H., Lafferty, J., and Wasserman, L. (2009), “The Nonparanormal, Semiparametric Estimation of High Dimensional Undirected Graphs,” *Journal of Machine Learning Research*, 10, 2295–2328. [595]
- Meinshausen, N., and Bühlmann, P. (2006), “High-Dimensional Graphs and Variable Selection With the Lasso,” *The Annals of Statistics*, 34, 1436–1462. [595,598,599]
- Ravikumar, P., and Wainwright, M. (2009), “High-Dimensional Ising Model Selection Using l_1 -Regularized Logistic Regression,” *The Annals of Statistics*, 38, 1287–1319. [602]
- Ravikumar, P., Wainwright, M., Raskutti, G., and Yu, B. (2008), “High-Dimensional Covariance Estimation by Minimizing l_1 -Penalized Log-Determinant Divergence,” Technical Report 797, UC Berkeley, Statistics Dept. [594,596-598,602]
- Rothman, A., Bickel, P., Levina, E., and Zhu, J. (2008), “Sparse Permutation Invariant Covariance Estimation,” *Electronic Journal of Statistics*, 2, 494–515. [594,599,602]
- Wu, W. B., and Pourahmadi, M. (2003), “Nonparametric Estimation of Large Covariance Matrices of Longitudinal Data,” *Biometrika*, 90, 831–844. [594]
- Yuan, M. (2009), “Sparse Inverse Covariance Matrix Estimation via Linear Programming,” *Journal of Machine Learning Research*, 11, 2261–2286. [594,595]
- Yuan, M., and Lin, Y. (2007), “Model Selection and Estimation in the Gaussian Graphical Model,” *Biometrika*, 94, 19–35. [594,602]
- Zhang, C. (2010), “Estimation of Large Inverse Matrices and Graphical Model Selection,” technical report, Rutgers University, Dept. of Statistics and Biostatistics. [602]
- Zhou, S., Lafferty, J., and Wasserman, L. (2010), “Time Varying Undirected Graphs,” *Machine Learning*, 80, 295–319. [602]
- Zhou, S., van de Geer, S., and Bühlmann, P. (2009), “Adaptive Lasso for High Dimensional Regression and Gaussian Graphical Modeling,” preprint, available at [arXiv:0903.2515](https://arxiv.org/abs/0903.2515). [599]